EVALUATION OF LOAD TRANSFER IN THE CELLULOSIC-FIBER/ POLYMER INTERPHASE USING A MICRO-RAMAN TENSILE TEST*

William T. Y. Tze†
Assistant Professor
Department of Bioproducts and Biosystems Engineering
203 Kaufert Laboratory, University of Minnesota
2004 Folwell Avenue
St. Paul, MN 55108

Shane C. O'Neill
Wood Plastic Composite Specialist
Advanced Engineered Wood Composites Center
5793 AEWC Building, University of Maine
Orono, ME 04469-5793

Carl P. Tripp
Professor
Laboratory for Surface Science and Technology
5708 ESBR-Barrows, University of Maine
Orono, ME 04469-5708

Douglas J. Gardner†
Professor

and

Stephen M. Shaler†
Professor and Co-Director
Advanced Engineered Wood Composites Center
5793 AEWC Building, University of Maine
Orono, ME 04469-5793

(Received February 2005)

ABSTRACT

The objectives of this research were (1) to use a Raman micro-spectroscopic technique to determine the tensile stress distributions of a cellulosic-fiber/polymer droplet interphase, and (2) to examine if the stress profile could be used to evaluate load transfer in fiber/polymer adhesion. Cellulosic fibers were treated with various silanes (amino, phenylamino, phenyl, and octadecyl functionalities) and a styrene-maleic anhydride copolymer to create different interphases upon bonding with polystyrene. A single fiber, bonded with a micro-droplet of polystyrene in the mid-span region of its gage length, was strained in tension. Raman spectra were collected at five-micrometer intervals along the embedded region of the fiber. The stress-dependent peak of cellulose (895 cm^{-1}) was analyzed for frequency shift so that the local tensile stress in the interface region could be determined. Results showed that the local tensile stresses of the strained fiber were lower in the embedded region compared to the exposed region, suggesting a transfer of load from the fiber to the matrix polymer. A deeper and sharper decline of the stress profile was observed when the fiber/droplet interaction was enhanced. Further analyses, involving conversion of

* The research reported in this paper was part of Dr. Tze's dissertation work (at the University of Maine), for which he won 2nd place in the 2004 Wood Award.

† Member of SWST.

Wood and Fiber Science, 39(1), 2007, pp. 184 – 195

tensile stress profiles to shear stress distributions in the interphase, confirmed that the micro-Raman/tensile test can be employed to evaluate fiber/matrix interfacial bonding in composites. This success signifies the possibility of evaluating adhesion between cellulosic fibers and brittle polymers, which is difficult to study using common micromechanical tests. Use of the micro-Raman technique can improve our understanding of wood/polymer adhesion.

Keywords: Raman spectroscopy, micromechanical test, cellulose fibers, polymer, interphase, load transfer, adhesion, silane.

INTRODUCTION

Wood-plastic composites (WPC) have been increasingly favored over the traditional wood products and the unfilled plastics for applications where structural requirements are low. Two examples of such applications are decking and window profiles. For railings and decking, WPCs, being more environmental-friendly, are partially replacing lumber treated with chromated copper arsenate (Smith 2001). In window applications, wood-filled poly(vinyl chloride) composites are gaining wide acceptance because they are more moisture-resistant compared to wood products, and are stiffer and more thermally stable compared to the unfilled plastics (Defosse 1999).

The common fillers for WPCs have been in the form of wood flour, but high-purity, stiff cellulose fibers are recently receiving much attention for producing engineered wood-plastic composites that have an enhanced structural performance compared to the conventional WPCs. Chemical pulp fibers ($\geq$95% alpha-cellulose content) have been used to reinforce engineered plastics such as nylon 6 at a fiber loading of 30–33% (Sears et al. 2002). The resulting composites exhibited properties that were intermediate between the wollastonite-reinforced nylon and the glass fiber-reinforced nylon. Apart from natural fibers, continuous regenerated cellulose (lyocell) fibers solvent-spun from wood pulp have also been used as a reinforcing agent for plastics. When combined with cellulose acetate butyrates, a naturally derived plastic, the resulting lyocell/polymer composites attained a stiffness modulus that exceeded 20 GPa (Franko et al. 2001).

As the WPC applications shift to end-uses of higher performance, it is increasingly important to engineer the composites, and such a need can be fulfilled with an improved understanding of the factors that influence the composite mechanical properties. The mechanical properties of fiber/polymer composites depend on the properties of the fiber, the matrix polymer, and the interphase, as well as the distribution behavior of the fibers in the matrix such as fiber volume fraction, orientation, and agglomeration (Hoecker and Karger-Kocsis 1996). While the mechanical properties of bulk fibers and matrix polymers are usually well known, the interface region (interphase), whose properties are different from the combining constituents, are not well understood. Therefore, much effort has been placed on studying the mechanical properties of the fiber/polymer interphase, and relating these properties to the composite performance.

A common approach for evaluating fiber/matrix interfacial properties is to evaluate the effectiveness of load transfer across the interface. For such a task, micro-composite tests are better than bulk mechanical tests whose results could be perturbed by fiber volumetric and orientation effects (Fan et al. 1991). The current micro-composite test methods, however, suffer particular limitations. In the micro-debond test (Fig. 1a), the interfacial shear strength is determined by shearing a polymer droplet from the fiber (Gaur and Miller 1989). However, this test is of limited use when the fiber is either too thin or too weak, or the interphase is too strong, thereby causing the fiber to break before shear removal of the droplet. In the fiber fragmentation test (Fig. 1b), the interfacial shear strength is deduced from the number (or length) of fiber fragments when a fiber-embedded polymer sample is subjected to a tensile load (Herrera-Franco and Drzal 1992). Unfortunately, this test

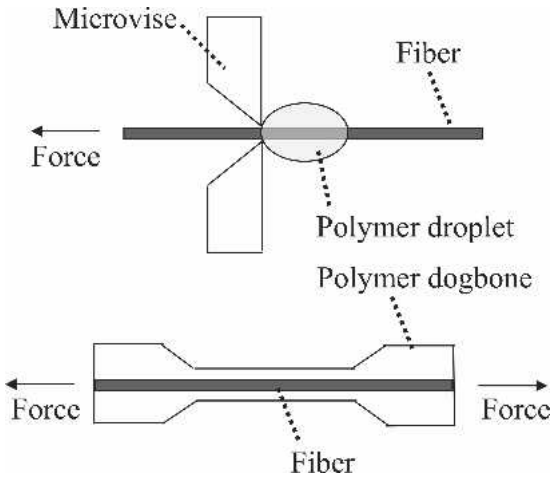

FIG. 1. Two common micro-composite tests: (a) the micro-debond test (top figure) and (b) the fiber fragmentation test (bottom figure).

cannot be applied to a brittle matrix polymer because the polymer will fracture before fiber fragmentation is observed.

Evaluation of interphases that are formed between cellulosic fibers and brittle polymers is challenging. Liu et al. (1996) performed micro-debond tests on wood-fiber/polystyrene interphases. They reported that 55% of the total samples tested in their study failed in fiber breakage and 5% in matrix cracking. Trejo-O'Reilly et al. (2000) employed fiber fragmentation tests for their lyocell-fiber/polystyrene system. They carried out the tests at 94°C, which is near the glass-transition temperature of polystyrene, presumably aiming to reduce the brittleness of the matrix polymer by testing the rubbery state. These researchers obtained the interfacial shear strength values, but did not obtain information about fiber/polymer interactions in the glassy state of the matrix, which may be more relevant to the normal use of the composites.

In addition to the stringent requirements for fiber/polymer combinations, the current micro-composite tests are also limited in identifying local strain or stress values that are critical to the prediction of failures in the fiber/polymer interphase. In the micro-debond test, for example, the maximum load to shear-off the droplet is averaged over the area of contact between the fiber and the matrix (Gaur and Miller 1989). The distribution of stress (or strain) in an interphase, however, is not uniform due to stress (or strain) concentrations. Because failures occur at locations of maximum stress or strain, depending upon the controlling failure criteria, the average state of the interphase may not accurately characterize the integrity of the interphase.

The strain or stress distributions of wood fibers have been determined using several unconventional techniques, but these approaches are either limited in applications or not robust enough for different matrix polymers. Mott et al. (1996) strained single wood pulp fibers under an environmental scanning electron microscope (ESEM), and subsequently compared sequential images for surface displacement, which could be converted to microstrain distributions on the fiber surfaces. The advantage of this technique, however, could not be fully utilized in fiber/polymer systems where the visibility of the fiber underlying the matrix polymer is greatly reduced. Mercado (1992) loaded in tension polyurethane samples that contained single wood fibers, and subsequently examined the image under a polarized microscope for birefringent pattern, whose light intensity is related to the stresses within the matrix polymer around the region of the fiber/polymer interphase. The technique, however, is primarily limited to transparent and birefringent matrix polymers (such as epoxy, polycarbonate, and polyester).

Raman micro-spectroscopy is a novel technique that provides a robust approach in identifying interfacial stress distributions for a potentially wide range of cellulose-fiber/polymer combinations. This technique relies on (1) identifying the stress-dependent vibrational frequency, (2) establishing the stress-frequency calibration curve, and (3) directly converting the frequency of a spectrum of interest to local stresses (Fig. 2). The stress-dependent Raman bands of cellulose have been identified by Eichhorn et al. (2001) to be at 895 cm^{-1} and 1095 cm^{-1}. These bands shift 0.4 cm^{-1} to lower frequencies for every 100 MPa increase in tensile stress. Therefore, if Raman bands are collected

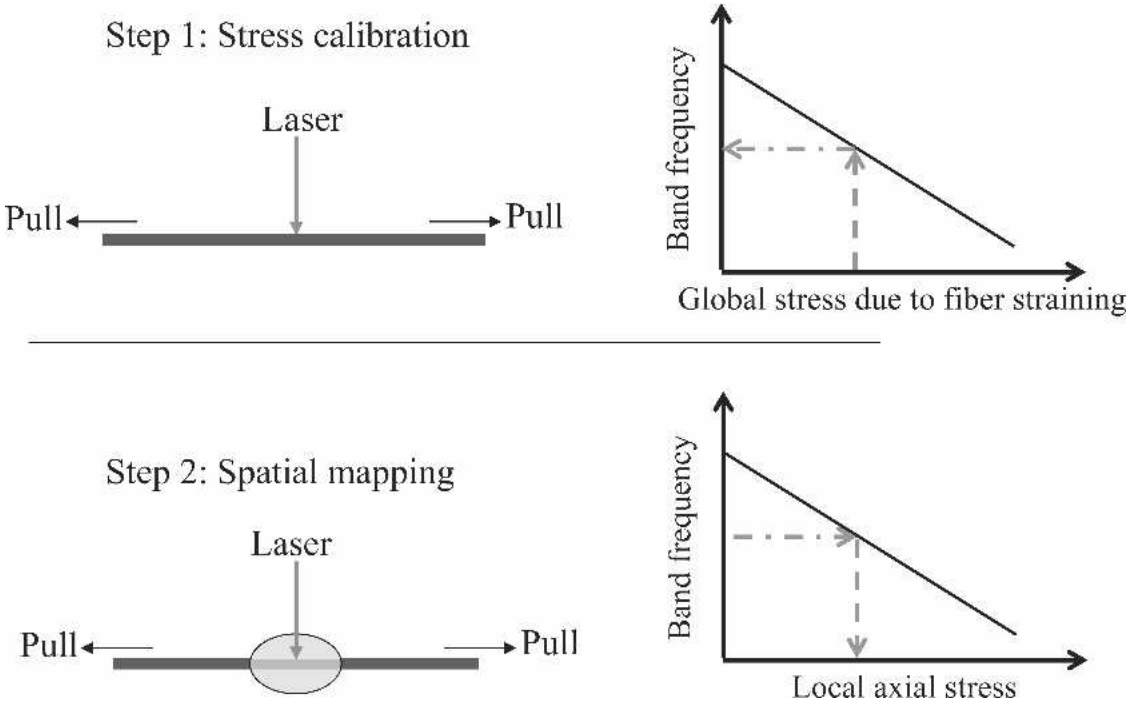

FIG. 2. A schematic approach of using Raman micro-spectroscopy for mapping tensile stress in the fiber/polymer interphase.

at different locations of the fiber along the region bonded with a matrix polymer, the point-to-point variation (or spatial distribution) of stress can thus be determined for the fiber/matrix interface region.

Research published so far indicates the promising applicability of the Raman technique in discerning strain and stress distributions in cellulosic-fiber/polymer interphases, but no practical success has been accomplished in evaluating interfacial bonding. In the absence of polymer matrices (or bonding), the Raman technique has been successfully employed to study microdeformation of natural cellulose (flax and hemp) fibers (Eichhorn et al. 2000) and to monitor the deformation process in regenerated cellulose (viscose and lyocell) fibers (Eichhorn et al. 2001). This technique was later extended to study fiber composites, where strain distribution was examined along the ends of a flax fiber embedded in an epoxy matrix (Eichhorn and Young 2003). In this study, however, no quantification was made regarding the extent of flax/epoxy bonding. In another investigation, the Raman technique was used to map the tensile stress distribution of single hemp fibers along the region bonded with an epoxy micro-droplet (Eichhorn and Young 2004). A maximum interfacial shear stress was identified, but the value approximated the shear yield stress of the epoxy resin, thereby implying a good adhesion but also a hampered attempt to quantify fiber/matrix adhesion.

The objectives of this study were (1) to systematically study stress distributions in the cellulosic-fiber/polymer interphase using a micro-Raman tensile technique, and (2) to examine if the stress profile could be used to evaluate load transfer in fiber/polymer adhesion.

MATERIALS AND METHODS

Test materials and equipment

The fibers used in this study were regenerated cellulose (lyocell) fibers solvent-spun from

wood pulp to a diameter of 12 micrometers. These fibers were acquired from Acordis Cellulosic Fibers (Tencel®) in the form of continuous fibers to increase the ease of sample handling. The fibers also have mechanical properties that are quite similar to mature (black spruce) wood fibers (Table 1). Polystyrene was used as the matrix polymer because it is a commonly available polymer. Additionally, polystyrene is a material of interest in this study because of its glassy (brittle) behavior, which has been known to cause complications in micromechanical tests. The polystyrene sample was of 125,000–250,000 weight-average molecular weight, and it was acquired from PolySciences Inc. The trialkoxysilanes used for fiber surface modification were of phenyl [$-C_6H_5$], amino [$-(CH_2)_3NH_2$], phenylamino [$-(CH_2)_3NHC_6H_5$], and octadecyl [$-(CH_2)_{17}CH_3$] functionalities, and they were acquired from Gelest, Inc. Styrene-maleic anhydride, another surface modifier used in this study, was a random diblock copolymer of 50/50 styrene and anhydride content based on percent weight (Polysciences Inc.). The copolymer had a number-average molecular weight of 1600 g/mol and an acid number of 480.

The Raman spectrometer (Renishaw system) used a diode laser operating at 785 nanometers (Fig. 3). The spectrometer was equipped with a microscope that could focus the laser beam to a spot size of 2 micrometers using a 50× objective lens (0.25 numerical aperture). A microtensile apparatus was placed under the microscope to hold or stretch a single fiber, and expose the fiber to the laser beam for collection of Raman spectra. The fiber holder of the apparatus had a moving arm at one side, and a stationary arm at the other side. The moving arm was actuated by a stepper motor via a leadscrew/nut system and gearhead, providing a linear motion of 0.1 micrometer repeatability. The motion was computer-controlled to attain a desired distance and speed for stretching the fiber. The stationary arm of the fiber holder was equipped with a strain-gage load cell of ±0.15% error (250 gram-force full scale). The stationary arm was also connected to a mini XY stage to position the fiber both horizontally and vertically prior to stretching. The microscope stage that held the tensile apparatus was another XY stage, which could be computer-programmed to position and move the tensile apparatus, and hence also the fiber, to allow spatial mapping at fixed intervals.

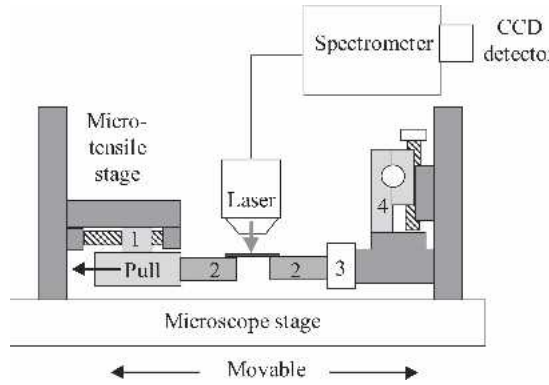

FIG. 3. The micro-Raman tensile test apparatus. Note: 1 = moving arm; 2 = fiber mounting arm; 3 = load cell; 4 = fiber aligning XY stage.

TABLE 1. *Some mechanical properties of regenerated cellulose and wood fibers.*

	Lyocell fibers[a]	Juvenile wood fibers[b]	Mature wood fibers[c]
Tensile modulus (GPa)	15.2	1.11	9.44
Ultimate tensile strength (GPa)	0.54	0.21	0.48
Strain at failure (%)	7	17[d]	6[d]

[a] Data from Eichhorn et al. (2001); 20 replicates; 83 μm/s.
[b] Data for 10-year old black spruce fibers (Egan and Shaler 2000); 18 replicates; 80 μm/s.
[c] Data for 55-year old black spruce fibers (Egan and Shaler 2000); 34 replicates; 80 μm/s.
[d] Data estimated from the stress-strain plots in Egan and Shaler (2000).

Sample preparation

Lyocell fibers were cleaned by Soxhlet-extraction for 12 hours using HPLC-grade methanol, and subsequently dried in an oven at 70°C until a constant weight was achieved. These fibers became either the control samples or the substrates for chemical treatments in this study.

For silane treatment, a 95 volume-% methanol solution was first acidified to pH 5 using acetic acid. Trialkoxysilane was then added to the

methanol solution at a dosage of 0.005 M, and let to hydrolyze for five minutes. For aminosilane, the pre-hydrolysis was performed in methanol solution that was not acidified. Fibers of about 2 grams (oven-dry weight) were soaked in the silane solution for 20 minutes at a temperature of 22°C and a relative humidity between 42–46%. Upon completion of the treatment, the residual chemical was rinsed off twice using HPLC-grade methanol. The rinsed fibers were heated in an oven at 110°C for 10 minutes and subsequently dried at 70°C for 24 hours to complete the crosslinking of the polymerized silane layers.

For grafting with styrene-maleic anhydride (SMA) copolymer, procedures were adopted from Liu (1994). First, 3.5 grams of copolymer were dissolved in 20 mL of N,N-dimethylformamide with 0.2% (based on the copolymer weight) of 4-dimethylaminopyridine as the catalyst. Then, about 0.5 grams of cellulose fibers were added to the solution to undergo the esterification reaction at 100°C for five hours. At the end of the reaction time, the fibers were rinsed twice using acetone, and subsequently extracted with acetone by Soxhlet for six hours. The extracted fibers were then dried at 70°C to evaporate the solvent.

For depositing polymer droplets onto the fibers, a 20 weight-% polystyrene solution in toluene was first prepared. A stiff fiber optic strand was used to transfer a drop of the polymer solution to the fiber, with an embedment length of 70–90 micrometers. The specimens were left in the fume hood for 18 hours to allow solvent to evaporate from the droplet. The evaporation was not assisted by heating so that thermal residual stresses in the fiber/polymer system could be avoided.

A single fiber, with an attached polymer droplet, was mounted onto the tensile stage with a gage length of 10 mm. The fiber was fixed to the stage at both ends using a five-minute curing epoxy. Although a fast-curing adhesive was used, a standing time of 18 hours was allowed to maximize curing so that fiber slippage could be minimized during tensile displacement. Under the assumption of no fiber slippage, the global strain of the fiber was considered similar to the nominal strain calculated from the ratio of displacement and the initial gage length.

Raman scanning

The fiber was loaded in tension at a rate of 10 micrometer/second to a strain level of 1%. The stretched fiber was then held in position for five minutes. Within this elapsed time, instantaneous stress relaxation occurred, as revealed in an initial study (Tze 2003), and any attempts made during the said period to examine the point-to-point (spatial) variation of stress (or the Raman band frequency) would be hampered by an additional source of variation: the time-dependent stress change. After the five-minute elapsed time, Raman spectra were collected at regular intervals of five micrometers along the droplet-embedded region of the fiber. Each Raman spectrum required 30 seconds to record. Upon completion of scanning, the fiber was further stretched, followed by a five-minute elapsed time and then spectra collection. The overall procedures were repeated for each loading level, which was in incremental steps of 1% strain (i.e., 1%, 2%, 3%, etc.).

The collected spectra consisted of cellulose and polystyrene bands (Fig. 4), and therefore these spectra were subtracted by the spectrum of polystyrene to produce cellulose spectra. The 895 cm^{-1} band of the cellulose spectrum was analyzed for frequency shift by curve fitting using a Laurentian:Gaussian ratio of 75:25. This frequency shift was then converted to the fiber

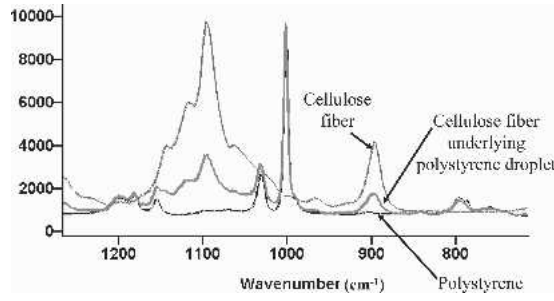

FIG. 4. The Raman bands of cellulose-fiber/polystyrene system and the individual components.

axial stress at a factor of 0.44 cm^{-1}/100 MPa, as determined in a prior calibration experiment (Tze 2003). All the calibration and Raman mapping experiments were carried out at 22 ± 1°C and 40 ± 3% relative humidity.

RESULTS AND DISCUSSION

Determining the tensile stress distribution in the fiber/polymer interphase

In the Raman tensile test approach, the local axial stress of the fiber embedded in a polymer droplet was determined from the frequency shift of the stress-sensitive band of cellulose. The band frequency shift, based on initial studies, was not affected by prolonged exposure to the laser beam of the Raman spectrometer, the solvent used for depositing the polymer droplet, nor the axial variation of the fiber (Tze 2003).

Figure 5 plots tensile stresses of the fiber as a function of distance from the center of embedment. When the fiber was unstrained, the tensile stresses in the fiber/polymer interphase did not differ from the local stresses of the fiber outside the droplet. When the fiber was stretched at 1% strain level, the local tensile stresses became lower in the embedded region compared to the exposed region, suggesting a transfer of load from the fiber to the embedding polymer. The fiber stresses declined from regions at both edges of the polymer droplet, and attained a minimum value near the mid-region of the embedment (Fig. 5). A similar stress profile was also obtained by Egan and Shaler (2000), who performed finite element analyses of a wood-fiber/phenol-formaldehyde droplet system with the fiber undergoing a tensile loading condition. Such an agreement lends merit to the empirical Raman approach, which has the advantage of not requiring mathematical assumptions on sample geometry and boundary conditions.

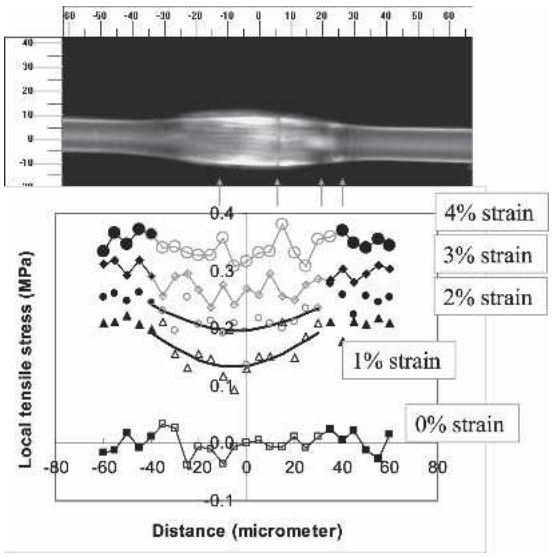

FIG. 5. The variation of fiber local tensile stress along the droplet-embedded region of the fiber and the corresponding polymer fractures in the sample.

The tensile stress as a function of distance along the droplet-embedded region of the fiber (Fig. 5) can be fitted using a fourth-order polynomial relationship to express the three inflection points: one each near the two edges of the droplet-embedded region, and the other one at the mid-region of the embedment. Such equations were satisfactory (R^2 or coefficients of determination not less than 0.80) for stress distribution profiles at 1% and 2% strain levels. For stretching at a higher strain level, the tensile stress distribution exhibited local variations in addition to the general trend of stress dissipation towards the mid-region of the embedment. The local tensile peak values corresponded to locations of polystyrene fractures (Fig. 5) that were observed to begin at 2% global strain level when the ultimate strain of polystyrene was attained. As such, the Raman technique is able to provide information of locally induced failures, which are not detected in numerical analyses.

Verifying load transfer in the fiber/polymer interphase

The next attempt of the study was to verify the load transfer phenomenon in the cellulose-fiber/polystyrene system. To demonstrate a case where no load transfer occurs, a micro-droplet of silicone fluid was applied onto single cellulose fibers. Silicone fluid is an inert compound that does not interact with cellulose, hence it presents

a fiber/polymer system where the interphase is not strong enough to transfer load, and the matrix (droplet) is not load-sustaining. To demonstrate a case where the load transfer ability is expected to be improved, cellulose fibers were treated with styrene-maleic anhydride (SMA) copolymer prior to forming a micro-bond with polystyrene. The copolymer has anhydride groups at one end to bond to cellulose and it has styrene groups at the other end to interact with polystyrene; hence it should facilitate load transfer in the fiber/polymer interphase.

Figure 6 depicts the stress distribution profiles for cellulose/silicone-fluid, cellulose/polystyrene, and cellulose-SMA/polystyrene systems at 1% applied strain. When no fiber/droplet interactions occurred (in cellulose/silicone-fluid system), the tensile stress profile did not show a noticeable decline along the embedded fiber. When the fiber/droplet interaction was enhanced (in cellulose-SMA/polystyrene system), the tensile stress profile exhibited a deeper decline towards the center of the droplet. Hence, the observed decline in the fiber tensile stress is an indication of fiber-to-matrix load transfer.

In brief, the tensile stress profiles determined from the micro-Raman tensile test are manifestations of load transfer phenomena in fiber/polymer composites. The transfer of loads reported here is from the fiber to the matrix. An interphase, however, should allow loads to transfer equally well either from the fiber to the matrix or the opposite direction. Therefore, the integrity of a bonding system, as inferred from this study, should be applicable to the matrix-to-fiber load transfer in relevance to the practical applications of fiber-reinforced composites.

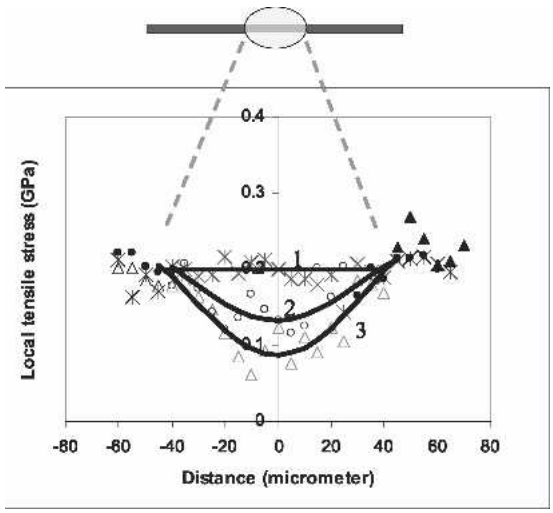

FIG. 6. Tensile stress distributions in three interphases at 1% global strain. Note: 1 = cellulose-fiber/silicon-fluid; 2 = cellulose-fiber/polystyrene, 3 = SMA-treated cellulose-fiber/ polystyrene. SMA refers to grafting with styrene-maleic anhydride copolymer.

Quantifying fiber/polymer interfacial bonding

The preceding discussion implies that tensile stress profiles in the fiber/polymer interphase could provide quantitative information of interfacial bonding. Indeed, the slope of a tensile stress profile has been related to interfacial shear strength for micro-debond (carbon/epoxy microcomposite) samples (Gu and Young 1997):

$$\tau = \frac{r}{2}\,\frac{d\sigma_f}{dx}, \tag{1}$$

where r is the fiber radius, and $d\sigma_f/dx$ is the slope of the tensile stress distribution curve at any point along the embedded fiber. Equation one was derived through the force balance approach, which is detailed in the appendix. The equation calculates the shear stress at any point along the embedded fiber. The values of $d\sigma_f/dx$ in the equation were determined from the slope of the regressed line (a fourth-order polynomial fitting) of the tensile stress profile. For such an analysis, the stress profile at 1% applied strain level was used so that the load dissipated in the embedded fiber was wholly converted to the shear force (as assumed for Eq. 1), but not partially expended on fracturing the polystyrene matrix.

The interfacial shear stress, as depicted in Fig. 7, is not uniform along the droplet-embedded region. The shear stress profile agrees with the finding of Eichhorn and Young (2004) for hemp/epoxy microbond in that (1) the interfacial shear stress value (the absolute value of τ) is maximum near regions where the fiber enters and exits the polymer droplet, and (2) the τ is zero

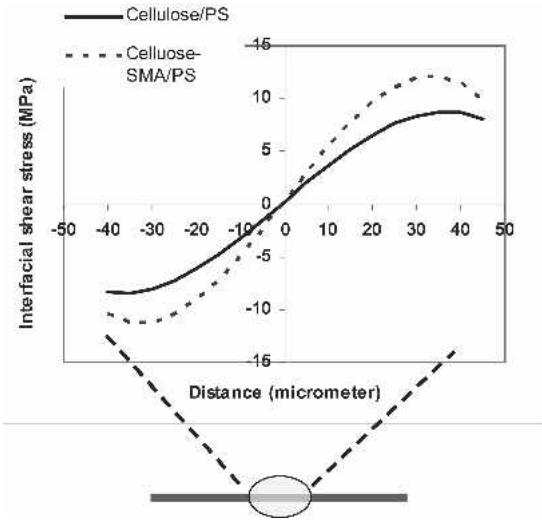

FIG. 7. Distributions of shear stress in the cellulose-fiber/polystyrene interphase for two systems of different fiber/matrix interactions at 1% applied strain.

near the mid-length of the embedment. Additionally, the present study identified, from the stress profile, maximum shear stress values (τ_{max}) of 8.7 MPa for the cellulose/polystyrene interphase and 12.1 MPa for the cellulose-SMA/polystyrene interphase. Such interfacial properties agree with the study of Liu et al. (1996), where macerated wood fibers were grafted with styrene-maleic anhydride copolymer using the same procedure and recipe used in this study. Based on the micro-debond test data, these researchers obtained interfacial shear strength values of 5.6 MPa for the (untreated) cellulose/polystyrene interphase and 10.0 MPa for the cellulose-SMA/polystyrene interphase. Presumably, these values would be higher and hence closer to our τ_{max} values (8.7 MPa and 12.1 MPa) if the micro-debond test, which was used by Liu et al. (1996), could take into account stress concentrations rather than average stress values.

Characterizing different types of interphases

This study has established that the tensile stress profiles of the embedded fiber can be used to quantify the fiber/polymer interfacial bonding. The subsequent attempt was to apply such knowledge to examine fiber/polystyrene systems whose interfacial chemistries were varied by pre-treating the fibers with different functional groups.

Figure 8 and Fig. 9 show the shear stress distributions obtained using the micro-Raman tensile tests. Treatments of fibers with a silane of alkyl (octadecyl) or non-polar functionality resulted in a fiber/polystyrene interphase of reduced shear stress (Fig. 8). This observation signifies that polar (acid-base) interactions are required in bonding fibers to a non-polyolefin polymer matrix. Adding polar (amino) functionality onto the fibers resulted in an increased shear stress (load transfer) in the fiber/polystyrene interphase, once again showing the importance of acid-base interactions. For fibers with induced phenyl groups (phenylamino-silanated, phenyl-silanated, and styrene copolymer esterified fibers), the resulting interphases exhibited a similar distribution of shear stress that is larger than the shear stress in the untreated fibers (Fig. 9). These observations indicate that the introduced phenyl group was the active group that inter-

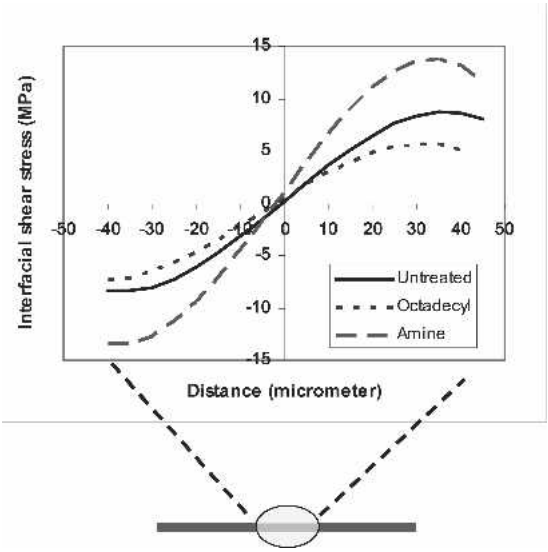

FIG. 8. Shear stress (at 1% applied strain) in the interphase between polystyrene and cellulose fibers treated with either non-polar (octadecyl-) or polar (amino-) functional silanes. Note: The data for untreated fibers were also plotted for comparison.

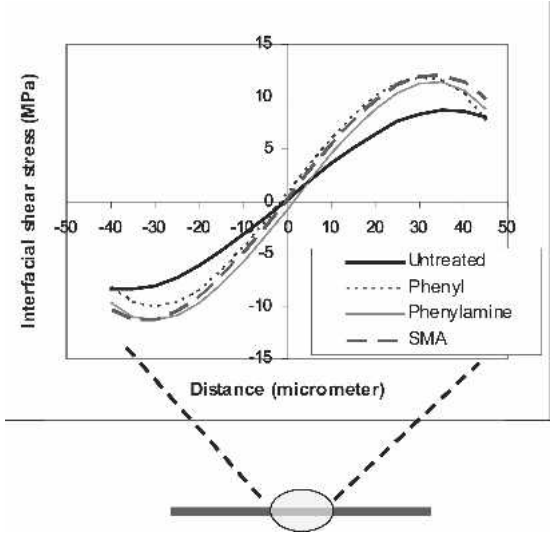

FIG. 9. Shear stress (at 1% applied strain) in the interphase between polystyrene and cellulose fibers treated with surface modifying agents that carry phenyl functionalities. Note: The data for untreated fibers were also plotted for comparisons.

acted with polystyrene, further demonstrating the importance of molecular compatibility in cellulose/polymer adhesion.

Overall, the micro-Raman tensile technique revealed maximum interfacial shear stress values of 8.0 to 13.8 MPa, in average, for the different interphases examined (Table 2). The data can be categorized to show ranking of the functional groups according to their adhesion to polystyrene: alkyl < untreated < phenyl = phenylamino = styrene copolymer < amino. These results demonstrate that the Raman technique is a powerful tool to examine cellulose/polymer adhesion and interphases.

TABLE 2. *Maximum interfacial shear stress (at 1% applied strain).*

Cellulose (Lyocell) fiber	Maximum interfacial shear stress, τ_{max} (MPa)
Untreated	9.3 ± 1.2 C
Amino-silanated	13.8 ± 1.8 A
Phenylamino-silanated	11.0 ± 2.0 B
Phenyl-silanated	11.8 ± 1.6 B
Octadecyl-silanated	8.0 ± 1.4 D
SMA-grafted	12.1 ± 1.6 B

The τ_{max} values in the table are averages obtained from six replicates. The variability (indicated by the ± sign) refers to the 95% confidence interval for the average value. The average values assigned with the same letters (i.e., A, B, C, or D) are not significantly different from one another at 95% confidence level, as tested based on the Student-Newman-Keul method using SigmaStat software. An exception is the statistical difference between the untreated and octadecyl-silanated fibers, whose confidence level is at 90%.

CONCLUSIONS

Raman spectra were collected at regular intervals of five micrometers along the droplet-embedded region of individual cellulosic fibers. The point-to-point variation of the cellulose band frequencies was converted to local tensile stress. A profile of local tensile stress was hence obtained as a function of distance along the droplet embedding length. The local tensile stress of the fiber exhibited a decline from the edge of the embedding region to the mid-length of the embedment. The stress decline was deeper and sharper for a stronger interphase. Therefore, the tensile stress profile obtained from the Raman tensile test demonstrates the phenomenon of load transfer where the load in the embedded fiber is dissipated to the matrix polymer. The slope of the stress profile along the droplet-embedded region allows for an estimation of the fiber/matrix interfacial shear stress. The shear stress value is maximum near regions where the fiber enters and exits the polymer droplet. The maximum (τ_{max}) shear stress values differed in different types of interphases, and the τ_{max} values increased when the fiber/polymer adhesion is stronger. Hence, the tensile stress profiles can be applied to evaluate fiber/polymer interfacial bonding.

Overall, this study demonstrates that Raman micro-spectroscopy can be employed to determine the tensile stress distributions of the cellulosic-fiber/polymer interphase and to evaluate load transfers in cellulosics/polymer adhesion. This technique characterizes bonding between a ductile fiber and a brittle polymer, which is difficult to study using common micromechanical tests. Although regenerated cellulose fibers were used in demonstrating the technique, its usefulness should also be applicable to wood fibers, which also contain cellulose. The success of the Raman technique also demonstrates the unique approach of applying a chemical tool (molecular vibrational spectroscopy) to the understanding

of mechanical properties of a cellulosic-fiber/polymer interphase.

ACKNOWLEDGMENTS

This research was financially supported by the USDA/CSREES New England Wood Utilization Research Fund (grant number ME-1999-05244). The fiber samples used in this study were donated by Acordis Cellulosic Fibers Inc., AL, USA.

REFERENCES

DEFOSSE, M. 1999. Processors focus on differentiation in window profiles. Modern Plastics Sept.:74–79.

EGAN, A., AND S. M. SHALER. 2000. Fracture and mechanics of fracture for resin coated single wood fibers. Pages 95–103 *in* G. Hague, M. McLauchlin, and T. Skinner, eds. Proc. Fourth European Panel Products Symposium, October 11–13, 2000, Llandudno, UK. The Biocomposites Centre, Bangor, UK.

EICHHORN, S. J., AND R. J. YOUNG. 2003. Deformation micromechanics of natural cellulose fibre networks and composites. Comp. Sci. Technol. 63:1225–1230.

———, AND ———. 2004. Composite micromechanics of hemp fibres and epoxy resin microdroplets. Comp. Sci. Technol. 64:767–772.

———, M. HUGUES, R. SNELL, AND L. MOTT. 2000. Strain induced shifts in the Raman spectra of natural cellulose fibers. J. Mater. Sci. Lett. 19:721–723.

———, R. J. YOUNG, AND W.–Y. YEH. 2001. Deformation processes in regenerated cellulose fibers. Text. Res. J. 71(2):121–129.

FAN, C. F., D. A. WALDMAN, AND S. L. HSU. 1991. Interfacial effects on stress distribution in model composites. J. Polym. Sci. Polym. Phys. 29:235–246.

FRANKO, A., K. C. SEAVEY, J. GUMAER, AND W. G. GLASSER. 2001. Continuous cellulose fiber-reinforced cellulose ester composites III. Commercial matrix and fiber option. Cellulose 8:171–179.

GAUR, U., AND B. MILLER. 1989. Microbond method for determination of the shear strength of a fiber/resin interface: Evaluation of experimental parameters. Comp. Sci. Technol. 34:35–51.

GU, X., AND R. J. YOUNG. 1997. Deformation micromechanics in model carbon fiber reinforced composites. Part II. The microbond test. Text. Res. J. 67(2):93–100.

HERRERA-FRANCO, P. J., AND L. T. DRZAL. 1992. Comparison of methods for the measurement of fiber/matrix adhesion in composites. Composites 23:2–27.

HOECKER, F., AND J. KARGER-KOCSIS. 1996. Surface energetics of carbon fibers and its effects on the mechanical performance of CF/EP composites. J. Appl. Polym. Sci. 59:139–153.

LIU, P. F. 1994. Characterizing interfacial adhesion between wood fibers and a thermoplastic matrix. Ph.D. dissertation, West Virginia University, Morgantown, WV. 170 pp.

———, T. G. RIALS, M. P. WOLCOTT, AND D. J. GARDNER. 1996. Interactions between wood fibers and amorphous polymers. Pages 74–81 *in* Proc. Woodfiber-Plastic Composites: Virgin and recycled wood fiber and polymers for composites, May 1–3, 1995, Madison, WI. Forest Prod. Soc., Madison, WI.

MERCADO, J. 1992. Using digital image analysis to determine the reinforcement of wood fiber polyurethane composites. MS. Thesis, Michigan Technological University, Houghton, MI. 71 pp.

MOTT, L., S. M. SHALER, AND L. H. GROOM. 1996. A technique to measure strain distributions in single wood pulp fibers. Wood Fiber Sci. 28(4):429–437.

SEARS, K. D., R. JACOBSON, D. F. CAULFIELD, AND J. UNDERWOOD. 2002. Reinforcement of engineering thermoplastics with high purity wood cellulose fibers. Pages 27–34 *in* Proc. Sixth International Conference on Woodfiber-Plastic Composites, May 15–16, 2001, Madison, WI, Forest Prod. Soc., Madison WI.

SMITH, P. M. 2001. U.S. woodfiber-plastic composite decking market. Pages 13–17 *in* Proc. Sixth International Conference on Woodfiber-Plastic Composites, May 15–16, 2001, Madison, WI. Forest Prod. Soc., Madison WI.

TREJO-O'REILLY, J. A., J. Y. CAVAILLÉ, M. PAILLET, A. GANDINI, P. HERRERA-FRANCO, AND J. CAUICH. 2000. Interfacial properties of regenerated cellulose fiber/polystyrene composite materials. Effect of the coupling agent's structure on the micromechanical behavior. Polym. Compos. 21(1):65–71.

TZE, W. T. Y. 2003. Effects of fiber/matrix interactions on the interfacial deformation micromechanics of cellulose-fiber/polymer composites. Ph.D. dissertation, University of Maine, Orono, ME. 191 pp.

APPENDIX

In the force balance approach adopted by Gu and Young (1997), the change in tensile force in the fiber is balanced by the change in shear force at the interface (see Fig. A1):

$$dF = 2\pi r\tau dx, \qquad \text{(A1)}$$

where F, r, τ, and x, respectively, refers to the tensile force on the fiber, the fiber radius, the shear stress at the fiber/polymer interface, and the position along the fiber in the embedded re-

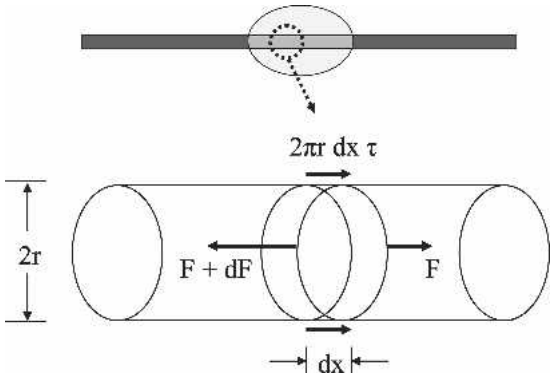

FIG. A1. Balance of tensile forces on an element of the fiber embedded in the polymer.

gion. Equation A1 can be simplified in terms of interfacial shear stress (τ):

$$\tau = \frac{1}{2\pi r}\,\frac{dF}{dx}. \tag{A2}$$

Because fiber tensile stress (σ_f) is the amount of tensile force (F) acting on a unit of fiber cross-sectional area (πr^2), a simple expression can be made:

$$dF = \pi r^2 d\sigma_f. \tag{A3}$$

The interfacial shear stress, after inserting Eq. A3 to Eq. A2, becomes:

$$\tau = \frac{1}{2\pi r}\,\frac{\pi r^2 d\sigma_f}{dx}, \quad \text{or} \quad \tau = \frac{r}{2}\,\frac{d\sigma_f}{dx}. \tag{A4}$$